Application of Image Reconstruction Techniques to Mars Neutron Spectroscopy Data

Meredith Curtis
NASA Undergraduate Research Program (USRP)
Los Alamos National Laboratory
Advisor, Thomas H. Prettyman
Rochester Insititute of Technology
Advisor, Carl Salvaggio
26-Feb-2009

Abstract

Data sets collected by the Mars Odyssey Neutron Spectrometer contain artifacts from spatial blurring and noise, which are limiting factors in the interpretation of surface physical properties. The spatial response of the spectrometer is about 10 degrees (full width half maximum) of arc length, making comparisons to and synthesis with higher resolution optical data sets and geological maps challenging. In addition, blurring artifacts can cause significant errors in the derived surface properties. Properties constrained by neutron spectroscopy include the abundance of water equivalent hydrogen (WEH), the column abundance of CO_2 in the seasonal caps, and the abundance of elements such as Fe and Cl, which have large cross sections for thermal neutron absorption. Computer codes were developed to reconstruct maps of the Martian surface with reduced blurring and noise, which can be subjected to geochemical interpretation with greater reliability. Penalty function and iterative deconvolution techniques (Jansson's method) were implemented and compared using simulated and measured data sets. These techniques were applied to global reconstruction of the Mars neutron spectroscopy data set. Both techniques were effective in removing noise without introducing unrealistic oscillations in the reconstructed maps. Results of the study are presented along with implications to Mars science.

I. Introduction

The Mars Odyssey Neutron Spectrometer was sent into space in 2001 where it sampled the Martian Surface for a duration of two Mars years. The spectrometer (Figure 1.) uses four boron-loaded plastic scintillators to detect neutrons. The use of a Cd-filter, self-shielding, and spacecraft motion enable the spectrometer to separately measure fast, epithermal, and thermal neutrons. The spectrometer measures the leakage spectrum of neutrons produced by the interaction of energetic particles and galactic cosmic rays with the surface and atmosphere of Mars [*Prettyman, 2006*]. The spectrometer is sensitive to neutron absorbing elements (such as Fe and Cl), the abundance and stratigraphy of water, and the column abundance of CO_2 ice in the seasonal polar caps.

Image reconstruction techniques were investigated to reduce spatial blurring and noise found in neutron spectroscopy data, which is used to globally map the composition of the Martian surface to depths of about 1 m. The data used in the following techniques was acquired from the P1 detector which contains a spatial resolution of 10° full width half max, and resembles that of a Gaussian distribution. When interpreting the counting rates from the p1 detector there are two issues that must be accounted for. First of all the data has been blurred due to the broad spatial response of the spectrometer, the data is also noisy due to the random nature of counting experiments. Spatial blurring and noise can distort surface features, leading to errors in the determination of surface physical properties. Several algorithms have been developed to minimize the artifacts that were created due to blur and noise. One dimensional iterative deconvolution techniques (Jansson's method), as well as deconvolution techniques containing a penalty function were implemented and compared using simulated and measured data sets.

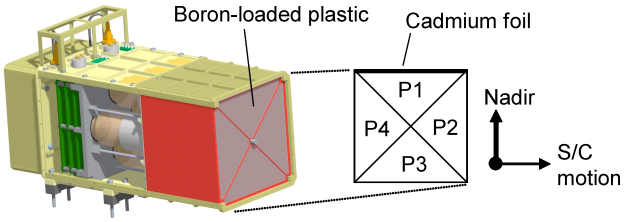

Figure1. Mars Odyssey Neutron Spectrometer

II. Jansson's Method

Jansson's method [*Jansson, 1997*] is an iterative deconvolution technique that uses smoothed data in order to try to obtain a new image for one dimensional meridian variation. The objective of spatial deconvolution is to enhance the spatial contrast, resolution, and information density of image data to the limit allowed by the uncertainty of the data [*Lawrence et al., 2007*]. This technique obtains smooth data by convolving the original data (d) with a Gaussian smoothing function (s). An image model is then found for the data by means of a double convolution of the image (i) convolved with a Gaussian function (s), and then convolved with the P1 response function (R), plus the average pixel standard deviations (ε) as seen below.

$$d = (i \otimes s) \otimes R + \varepsilon \qquad \text{Image model}$$

$$i^{k} = i^{k-1} + \Theta^{k-1}\delta^{k-1} \qquad \text{Iterative}$$

$$\delta^{k-1} = d - (i^{k-1} \otimes s) \otimes R$$

$$\Theta_{i}^{k-1} = \kappa[1 - (\frac{2}{i_{\max}})(i^{k-1} - \frac{i_{\max}}{2})] \qquad \text{Diagonal relaxation matrix}$$

A fixed number of iterations were carried out in order to sharpen the image. In the iterative equations seen above delta represents the difference between the image and the model, while theta keeps the function in bounds by use of a diagonal relaxation matrix. This method is illustrated in Figure 2 for data collected in early spring on Mars. Jansson's method was applied to the global data set in two dimensions. The deconvolved map enhances (sharpens) surface features; however, noise is also introduced, particularly at low latitudes where data coverage is sparse (Figure 2a). One of our main objectives is to determine whether Penalized Likelihood techniques will reduce noise artifacts in the reconstructed image. In this work, we use one-dimensional data sets (meridional cuts) to test our algorithms to simplify implementation and reduce the amount of time required to study variations in algorithm parameters. Algorithms that are found to be effective can be extended to two dimensions.

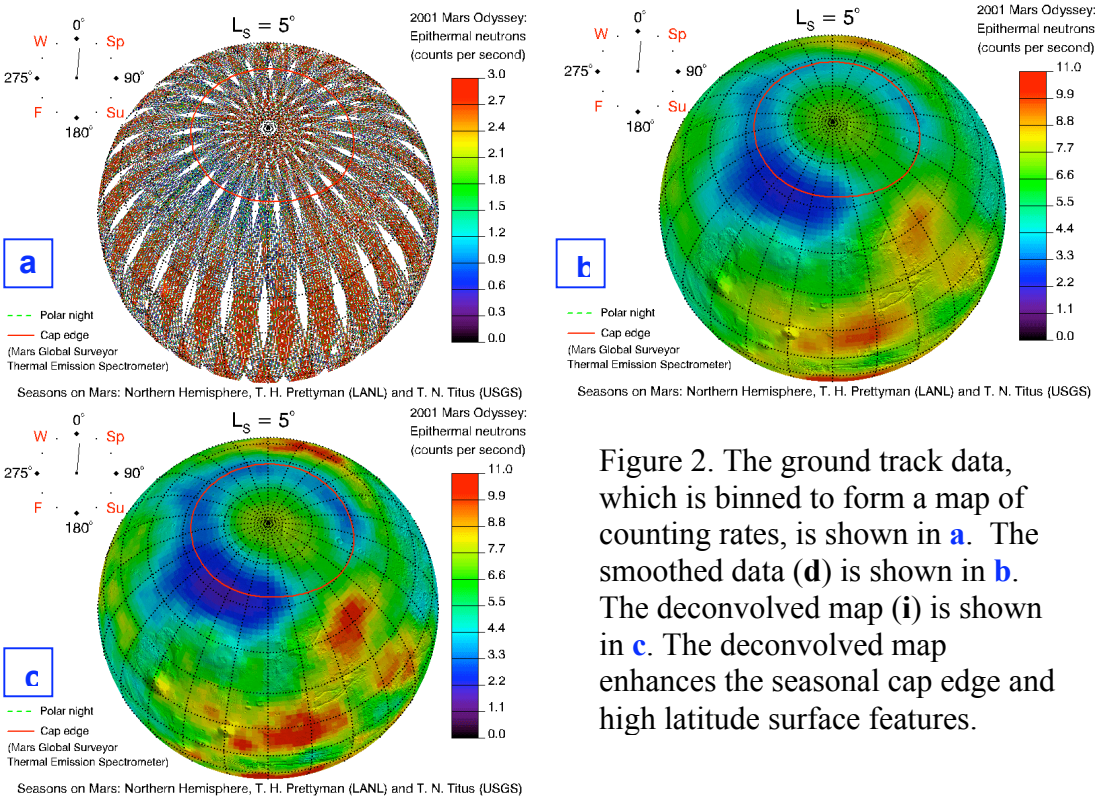

Figure 2. The ground track data, which is binned to form a map of counting rates, is shown in **a**. The smoothed data (**d**) is shown in **b**. The deconvolved map (**i**) is shown in **c**. The deconvolved map enhances the seasonal cap edge and high latitude surface features.

III. Penalized Likelihood

The goal of Penalized Likelihood is to find an image that is consistent with the data and that contains the least information content. Unlike Jansson's method, uncertainties in the data, both systematic and statistical, must be determined. The statistical contribution for each pixel was determined by calculating the variance in the mean counting rates for many overpasses of the pixel. The magnitude of systematic errors was determined by examining inter-pixel fluctuations and comparing them to the statistical uncertainty. The total uncertainty was determined by fitting a line to adjacent pixels on a scale less than the resolution of the spectrometer. Deviations from the line were used to measure the uncertainty.

Penalized likelihood calls for the minimization of some function f with respect to the image and data. This function contains two components, chi squared reduced χ^2_υ and a penalty function. Chi squared reduced is the weighted sum of the squares of the deviations between the model and the data, and makes sure that for every data pixel there is a corresponding model pixel. The model is found my convolving the original image with the P1 response function. The response function is determined by the counting rate of neutrons as a function of distance along the orbital path as the spectrometer passes over a point source of radiation on the Martian surface [*Prettyman, 2006*]. The penalty function consists of two terms, a penalty factor (λ) multiplied by the L2 norm of the Laplacian of the solution. These two terms add constraints to the data so that it is neither over nor under fitted. The penalty factor is found by plotting the penalty versus the

minimum of chi squared as seen in figure 3. In order for the deviations between the model and the data to be comparable to the uncertainty in the data the penalty factor is adjusted until chi squared reduced equals one.

$$\text{minimize } \mathrm{f}(\mathbf{i}|\mathbf{d}) = \chi_\upsilon^2(\mathbf{i},\mathbf{d}) + \lambda\left\|\nabla^2\mathbf{i}\right\|_2^2$$

$$\chi_\upsilon^2 = \frac{1}{n-1}\sum_{i=0}^{n-1}\frac{\left[d_i - (\mathbf{i}\otimes\mathbf{r})_i\right]^2}{\sigma_i^2}$$

$$m_i = \sum_{j=0}^{n-1} i_j \otimes R_{i-j+\frac{m-1}{2}}$$

If the penalty factor were to increase causing chi squared reduced to no longer equal one the penalty function would dominate causing the data to become overly smoothed until it resembled a flat line. If the penalty factor decreased chi squared reduced would dominate producing wild oscillations in the data. Figure 4 shows the data at 20° longitude that was analyzed using both methods.

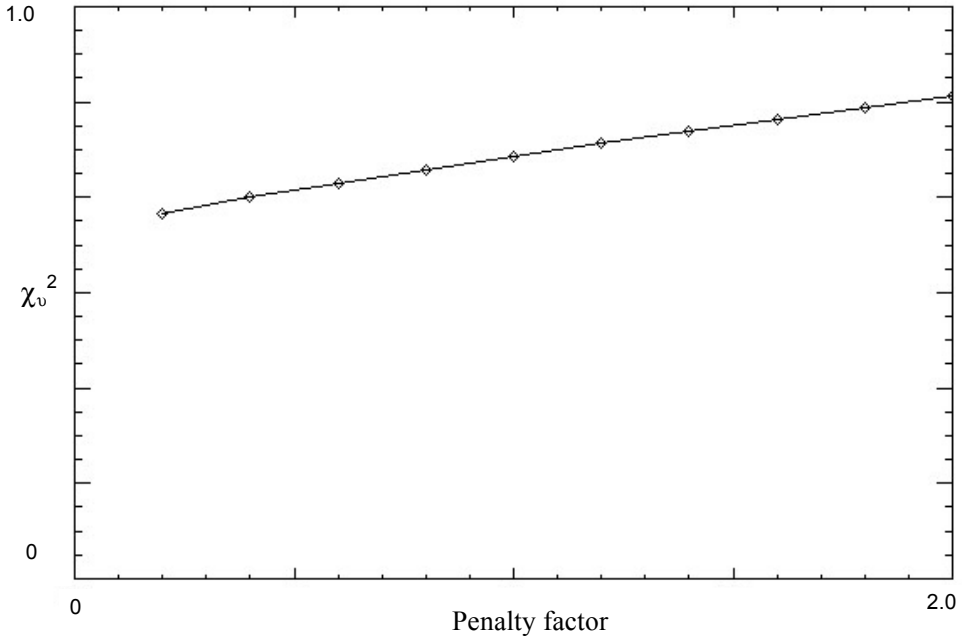

Figure 3. Penalty factor versus chi squared

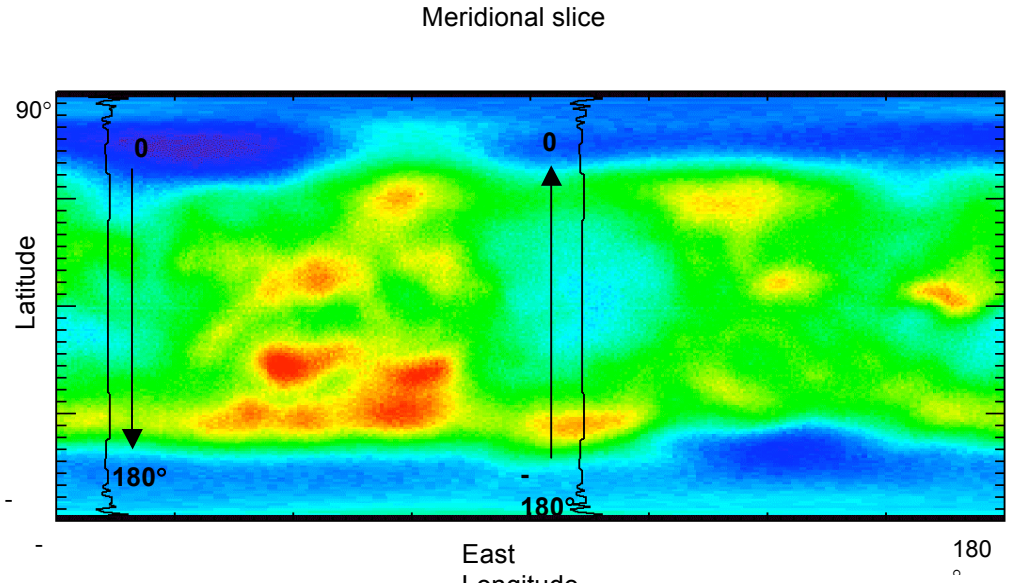

Figure 4. The surface of Mars demonstrating the selection of 20° longitude as a target area for further analysis.

IV. Qualitative Results

Both Jansson's method and the penalized likelihood method produced sharper images. However, Jansson's method allows for an unlimited number of iterations that can cause the data to be either over or under fitted. As the number of iterations increases the model will continue to deviate from the true image as shown in figure 5. An increasing amount of iterations also causes the noise to become magnified. Figure 6 demonstrates when the algorithm consists of 30 iterations. However, when 100 iterations where applied in Figure 7 the noise in the new image substantially increased.

The penalized likelihood method, on the other hand, was able to smooth and sharpen the image more effectively than Jansson's method. This is due to the fact that there is a criterion for the penalty function which adds constraints so that the model image is neither under nor over fitting the original data; however, in order for the algorithm to produce reliable results, accurate estimates of the uncertainties are needed. Figure 8 demonstrates the results using the Penalized likelihood deconvolution technique with a penalty factor of 1.81. The image is seen as being much smoother and contains less noise when compared to figure 6. Statistical and systematic errors were also considered in estimating the uncertainty for each pixel. The statistical uncertainty depends strongly on time duration (ΔL_S: areocentric longitude of the sun) over which the data were binned. Results shows that even for images produced with less data, and therefore greater statistical variations, a smooth image was still achieved (figure 9).

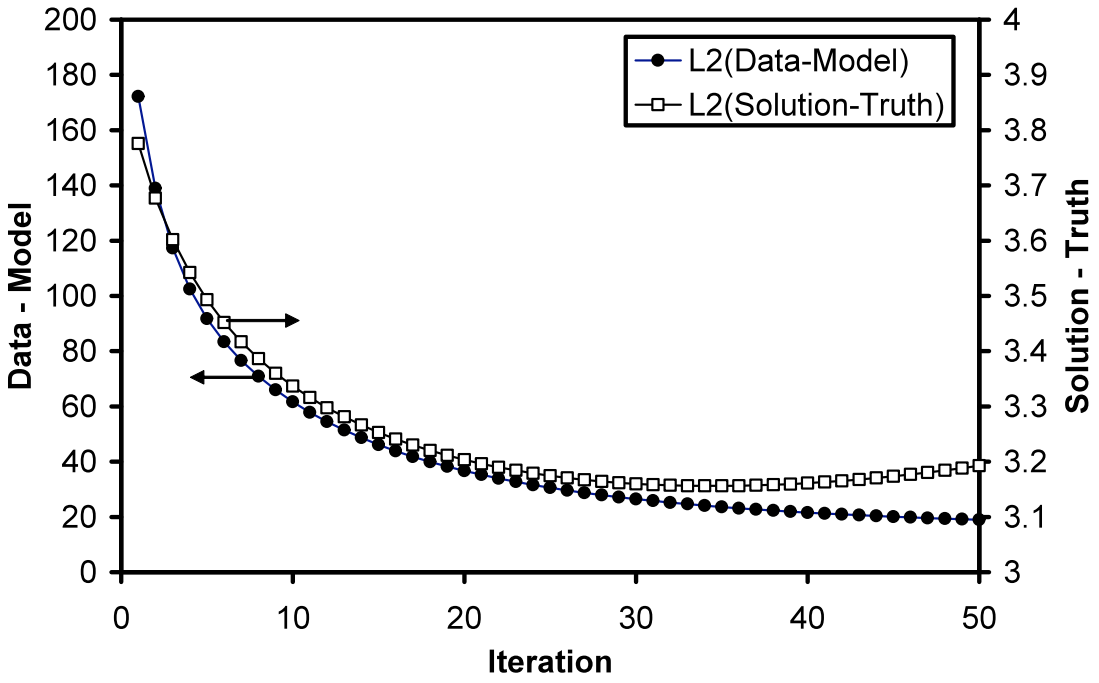

Figure 5. The graph above shows that while the difference between the data and model decreases as a function of iteration, there is clearly an optimal number of iterations beyond which the solution diverges from truth.

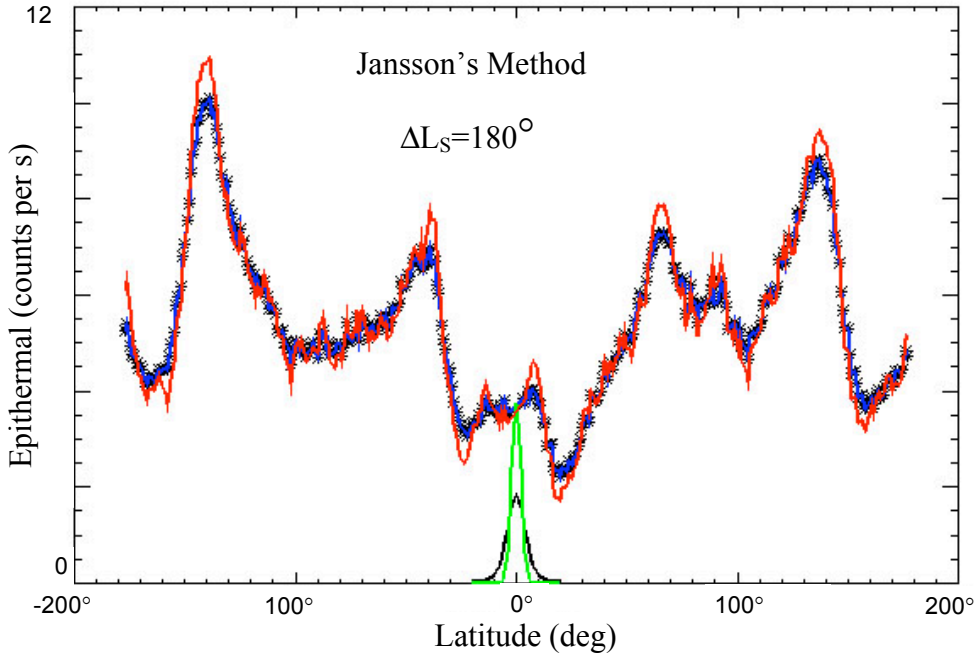

Figure 6. Meridional data are shown (above) as a blue line with symbols. The deconvolved map (**i**) is shown in red after 30 iterations. The smoothing function (**s**) is a

5° FWHM Gaussian, shown in green. The response function (**r**) is shown in black. (Jansson's method)

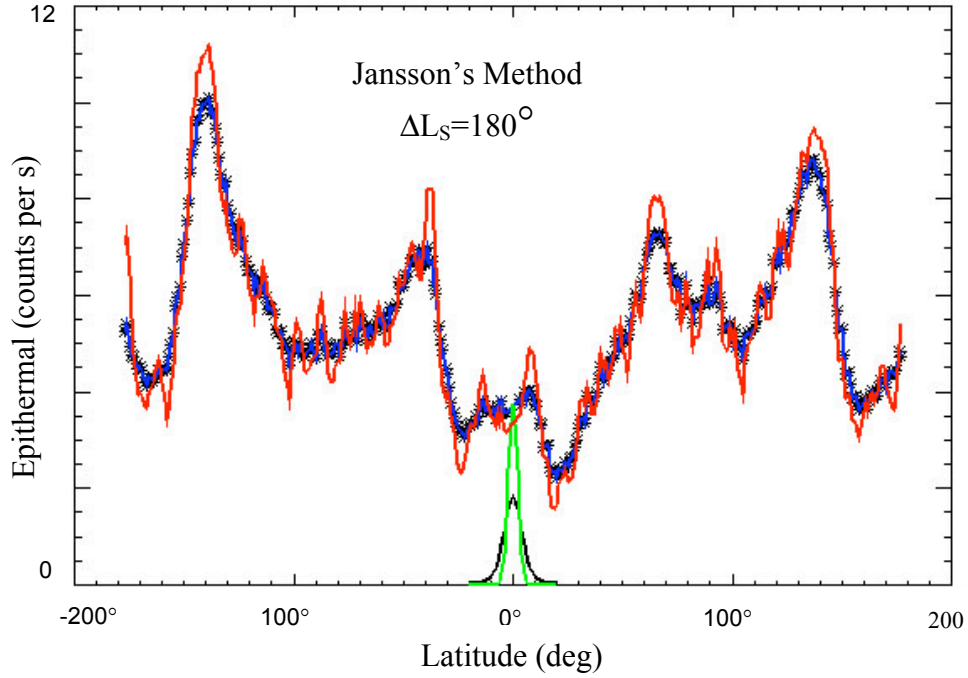

Figure 7. Meridional data are shown (above) as a blue line with symbols. The deconvolved map (**i**) is shown in red after 100 iterations. The smoothing function (**s**) is a 5° FWHM Gaussian, shown in green. The response function (**r**) is shown in black. (Jansson's method)

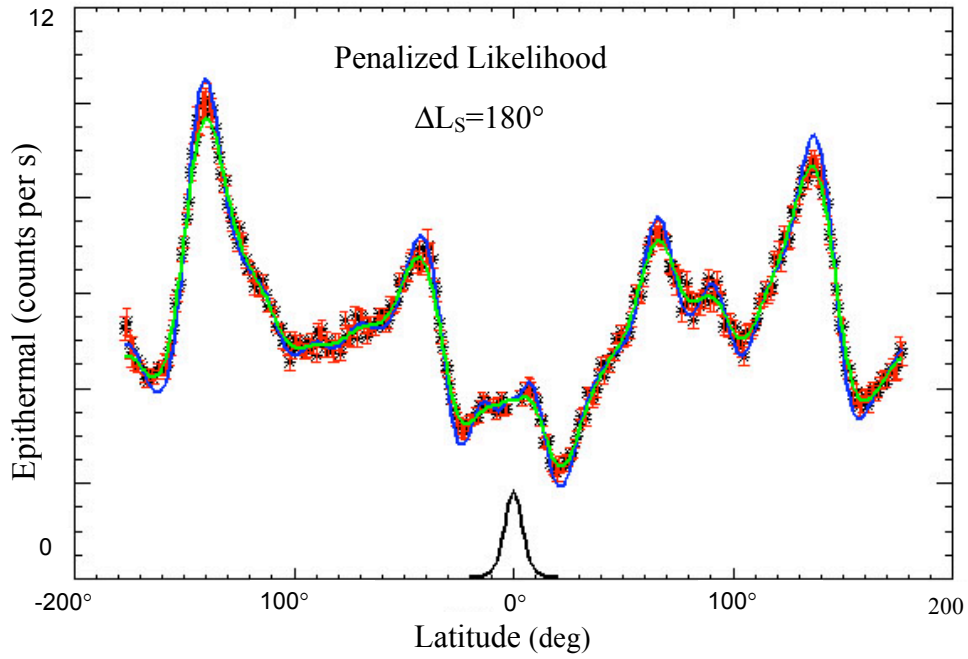

Figure 8. Meridional data are shown (above) as symbols with error bars. The deconvolved map (**i**) is shown in blue. The model **i**⊗**r** is shown in green. The response function (**r**) is shown in black. (Penalized likelihood)

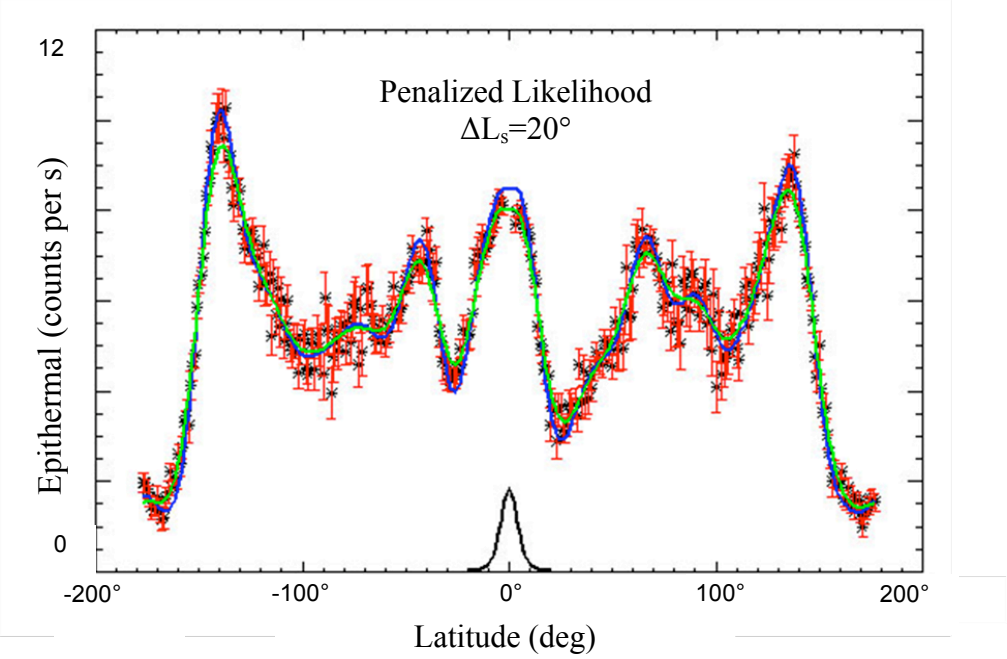

Figure 9. Data points for a ılated over 20° L_S.

Significance of regression and lack of fit were used to test the correlation between Jansson's and the penalized likelihood reconstructed maps with the original data. These tests take into consideration that linear regression equals one when there is perfect correspondence between the map and raw data, Figure 10. Significance of regression determines whether the slope computed for the data is significantly different than a slope of zero. The mean square due to regression (MS_{Reg}) divided by the mean square due to residual error (s^2) finds the result (F). Figure 11 and 12 demonstrate a result of greater than 1 illustrating a slope significantly different than zero. Lack of fit finds the difference between the reconstructed map and raw data by comparison to the mean value in the data. Result (F) is found by dividing the mean square due to lack of fit (MS_L) by the mean square due to pure error (S_e^2). If the result is less than 1 the model does not suffer from lack of fit. Figure 11 and 12 illustrate a lack of fit between the two reconstructed maps and original data. However, the map from penalized likelihood method shows a better fit to the data than the map from Jansson's method.

$$F = \frac{MS_{Reg}}{s^2} \qquad \text{Significance of Regression}$$

$$F = \frac{MS_L}{s_e^2} \qquad \text{Lack of Fit}$$

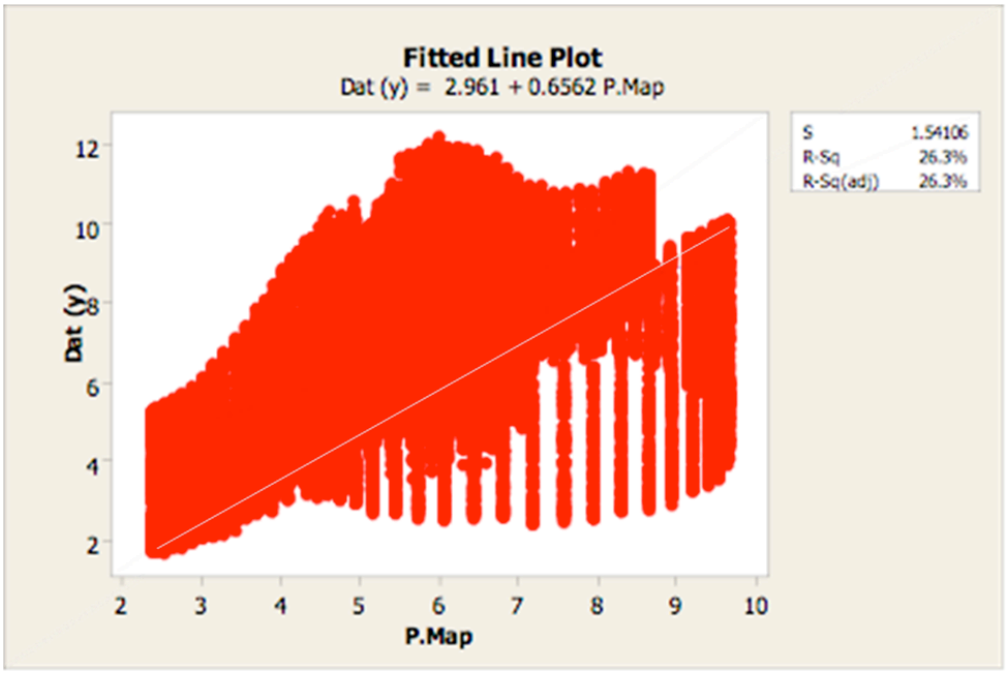

Figure 10. Linear regression, or lack thereof, is demonstrated by the penalized likelihood map (P. Map) versus the raw data (Dat).

Source	DF	SS	MS	F	P
Regression	1	31649	31649	12755.14	0.000
Residual Error	42667	105869	2		
Lack of Fit	348	50561	145	111.17	0.000
Pure Error	42319	55308	1		
Total	42668	137519			

Figure 11. Significance of regression and lack of fit results for Jansson's method.

Source	DF	SS	MS	F	P
Regression	1	36190	36190	15238.47	0.000
Residual Error	42667	101329	2		
Lack of Fit	348	46021	132	101.19	0.000
Pure Error	42319	55308	1		
Total	42668	137519			

Figure 12. Significance of regression and lack of fit results for Penalized likelihood method.

To compare Jansson's and the penalized likelihood method against one another a different approach was required due to the lack of replicates in the reconstructed maps. The two maps were thought of as cumulative density functions that were then changed into probability density functions by finding the derivative. Chi-squared goodness of fit test was then utilized. When the map from Jansson's method served as the observed PDF (O) and the map from the penalized likelihood method served as the expected PDF (E), chi squared was found to be 54621.03. Jansson's map then performed as the expected PDF and the penalized likelihood map became the observed PDF, resulting in a chi squared of 4.7×10^{7}. Compared to a chi squared statistic of 392.5 both calculated results were larger than the statistic. Therefore, the null hypothesis was rejected in each scenario, concluding that the two reconstructed maps are in fact different.

$$\chi^2 = \sum_{i=1}^{m}\left(\frac{O_i - E_i}{E_i}\right)^2$$

VI. Conclusion

Both Jansson's method and penalized likelihood deconvolution techniques produced sharper maps; however, the use of Jansson's method results in noise in the reconstructed map even for data accumulated over long periods of time (with minimal statistical variation). Penalized likelihood produces smooth, deconvolved maps even for data with large statistical variations. Penalized likelihood also adds constraints by the use of a penalty function so that the data is neither over nor under fitted, and takes into account statistical and systematic uncertainties.

We found that systematic errors in the data processing introduce local variations that persist even for large ΔL_S. Improvements in data processing are needed in order to realize the full potential of deconvolution methods.

Appendix: Measured and Simulated Data Algorithms

Mars Data Sets

Penalized Likelihood
SliceData2
gee2
dgee2
latsmooth2
convolution2
stand2

Jansson's Method
SliceData3
convolution3
Jansson

References

Draper, N.R., H. Smith (1981), Applied Regression Analysis. 2nd ed. New York: John Wiley & Sons, 31-40

Jansson, P.A., (1997), Deconvolution of Images and Spectra. 2nd ed. San Diego, CA: Academic Press, 119-134

Lawrence, D. J., R. C. Puetter, R. C. Elphic, W. C. Feldman, J. J. Hagerty, T. H. Prettyman, and P. D. Spudis (2007), Global spatial deconvolution of Lunar Prospector Th Abundances. *Geophys. Res. Lett.*, 34, L03201, doi:10.1029/2006GL028530

Prettyman, T. H., (2006), Remote chemical Sensing Using Nuclear Spectroscopy. Academic Press, 766-767